Journal of Applied Polymer Science

Silver-nanoparticle-incorporated composite nanofibers for potential wound-dressing applications

Poornima Dubey,[1] Bharat Bhushan,[1] Abhay Sachdev,[1] Ishita Matai,[1] S. Uday Kumar,[1] P. Gopinath[1,2]
[1]Nanobiotechnology Laboratory, Centre for Nanotechnology, Indian Institute of Technology Roorkee, Uttarakhand 247667, India
[2]Department of Biotechnology, Indian Institute of Technology Roorkee, Roorkee, Uttarakhand 247667, India
Correspondence to: P. Gopinath (E-mail: pgopifnt@iitr.ernet.in or genegopi@gmail.com)

ABSTRACT: The aim of this study was to develop stable and porous poly(ethylene oxide) (PEO)–polycaprolactone blended and silver nanoparticle (Ag NP) incorporated composite nanofiber scaffolds as antibacterial wound dressings. A facile approach for the *in situ* synthesis of Ag NPs was explored. In this synthesis method, *N,N*-dimethylformamide (DMF) was used as a solvent; it also acted as reducing agent for Ag NP formation. The stabilization of Ag NPs in the fibers was accomplished by PEO, which in turn acted as a reducing agent along with DMF. The successful synthesis of crystalline Ag NPs was confirmed by various characterization techniques. Thermogravimetric analysis, wettability, and surface roughness analysis of the nanofibers were done to examine the suitability of the scaffold for wound dressing. The as-synthesized composite nanofibers possessed good roughness, wettability, and antibacterial potential against recombinant green fluorescent proteins expressing antibiotic-resistant *Escherichia coli*. Thus, the nanofiber scaffold fabricated by this approach could serve as an ideal wound dressing. © 2015 Wiley Periodicals, Inc. J. Appl. Polym. Sci. **2015**, *132*, 42473.

KEYWORDS: applications; biomedical applications; composites; electrospinning; fibers

Received 23 December 2014; accepted 6 May 2015
DOI: 10.1002/app.42473

INTRODUCTION

In the recent past, there has been growing interest in the incorporation of metal nanoparticles into polymeric nanofibers for antibacterial applications.[1] One cost-effective, reproducible, and simple route for nanofiber fabrication is electrospinning. Electrospun nanofiber membranes can promote cell proliferation, differentiation, and migration; this has made them an ideal three-dimensional scaffold for tissue engineering over the last several years.[2] Nanofiber matrices have attracted significant attention lately for a variety of biomedical applications as they closely mimic the diameter of collagen fibrils in the natural extracellular matrix. Nanofibrous membranes possess several advantages over other wound-dressing materials. Nanofibers provide a high surface-area-to-volume ratio, microporosity, and ability for drug loading, and this makes them significant wound-dressing materials.[3]

Silver nanoparticles (Ag NPs) are well known for their antimicrobial activity against a wide spectrum of microbes; thus, they have been used in many biomedical applications, including burns, wounds, and other microbial infections; augmentation devices; tissue scaffolds; and antimicrobial filters.[4–7] They have been widely used in the preparation of various polymeric materials through their incorporation onto the surface as coatings or into composite materials for drug-delivery applications.[8] Successful antimicrobial activities of composite nanofibers containing Ag NPs have been reported with various polymers, including gelatin, poly(vinyl alcohol), poly(ethylene oxide) (PEO), and chitosan.[1,9–12]

In the recent past, polymeric blend materials incorporated with drugs have received great attention for their sustained and efficient drug delivery.[6] The antibacterial potential of Ag NP encapsulated PEO–polycaprolactone (PCL) polymeric blend nanofiber composite membranes has not been explored yet. PEO and PCL are biodegradable and biocompatible Food and Drug Administration approved polymers. Previously, PEO hydrogels were used for wound dressings, and PEO has also been used in several polymer blends as a wound-dressing material as it provides significant hydrophilicity to the membrane.[13] PCL has also been used in blends for wound-dressing applications as it provides mechanical strength to the dressing, and it is also a carrier for drugs in drug-delivery systems.[14] Thus, PCL could be used for the fabrication of blends to prevent the use of crosslinking or heat treatments, which could also hamper their properties.

Nevertheless, the effectiveness of Ag NPs gets hampered by agglomeration in biological systems.[15,16] Thus, for effective antibacterial activity, stable Ag NPs are of the utmost necessity. Thus, the aim of this study was to develop porous, stable, biocompatible, and biodegradable Ag NP incorporated nanofibrous composite membranes as antimicrobial wound dressings. The

synthesized nanofibers could be exploited as antibacterial wound dressings against a wide range of bacterial communities, such as *Staphylococcus aureus* and *Escherichia coli,* usually found in wounds. In this study, green fluorescent protein (GFP) expressing antibiotic-resistant *E. coli* was used to examine the antibacterial potential of the nanofibers. The presence of GFP allowed the rapid monitoring of bacterial growth inhibition by composite nanofibers. In the first part of the study, the *in situ* synthesis and characterization of Ag NPs in a PEO polymer solution were done. In the second part of the study, the synthesis of the composite nanofibers was done, and the antimicrobial potential of the membrane was assessed against antibiotic-resistant GFP *E. coli* bacteria.

EXPERIMENTAL

Materials

The PEO (viscosity-average molecular weight = 900,000) and PCL (viscosity-average molecular weight = 70,000–90,000) polymers were purchased from Sigma-Aldrich Co. *N,N*-Dimethylformamide (DMF) and methylene chloride were procured from Thomas Bakers, and silver nitrate ($AgNO_3$; 99%) and Luria-Bertani (LB) medium were obtained from Merck India. Agar–agar was procured from Himedia Laboratory, Ltd. (Mumbai, India). The recombinant GFP *E. coli* bacterial strain was prepared as reported previously.[17]

In Situ Synthesis of Ag NPs

In this study, we adopted the facile and novel approach for Ag NP synthesis by electrospinning the solution itself without any addition of external reducing or stabilizing agent. The synthesis was done in a high-molecular-weight PEO (molecular weight < 90,000) solution in Dichloromethane (DCM)–DMF (4 : 1 v/v), where $AgNO_3$ was soluble in the DMF phase, and the DCM/DMF solvent mixture was miscible. After 4–6 h of stirring, there was the generation of a yellow color; this confirmed the Ag NP formation.

Fabrication of the PEO–PCL Blended and Ag NP Loaded Nanofiber Mat (Composite Nanofiber)

Preparation of the Electrospinning Solution. PEO (4 wt %) and PCL (1 wt %) were dissolved in a 4 : 1 v/v DCM–DMF solvent mixture to prepare the solution for the electrospinning of the PEO–PCL blended nanofibers. Ag NPs synthesized in the PEO solution by the previously described method was mixed separately with a PCL solution in a 4 : 1 v/v DCM–DMF solvent mixture and stirred for 1 h to form a complete homogeneous solution. Different concentrations of PEO–PCL (1–4 wt %) were used for optimization of the bead-free nanofibers. Three different concentrations (1–3 wt %) of $AgNO_3$ were used for the fabrication of the Ag NP loaded nanofibers.

Nanofiber Fabrication. An electrospinning process was adopted for the fabrication of the nanofibrous membranes. Various parameters were optimized for the successful fabrication of the nanofibers.[18] The generation of ultrafine fibers was done in the presence of a high-voltage power supply (16–24 kV) to the metallic needle (18–21 G) attached to a 5-mL syringe at a feeding rate of 0.3 mL/h controlled by a syringe pump. A grounded electrode copper plate covered with aluminum foil with a thickness of 0.5 mm was used as a collector for nanofibers with a predetermined horizontal distance from the needle tip (10–16 cm). The electrospinning process was performed under ambient temperature conditions (25°C and 60% relative humidity). The generation of dried nanofibers was done during electrospinning because of the evaporation of volatile DCM solvent from the polymer solution toward the collector, so there was little need to dry the nanofibers. Further drying of the nanofibers was done in a desiccator in the presence of silica for the complete removal of a residual solvent. The PEO–PCL nanofiber without Ag NPs were denoted as alone PEO–PCL nanofibers and nanofibers with Ag NPs were denoted as composite nanofibers, respectively.

The optimized parameters used for fabrication are summarized as follows: 4 wt % PEO solution in a 4 : 1 v/v DCM–DMF solvent mixture, 1 wt % PCL, and 2 and 3 wt % $AgNO_3$ concentrations, 12-kV applied voltage, and 14-cm tip-to-collector distance of 14 cm, 0.3 mL/h solution flow rate, and 18-gauge blunt end tip needle.

Physicochemical Characterization of the Nanofibers

Ultraviolet–Visible (UV–vis) Spectroscopic and Transmission Electron Microscopy (TEM) Analysis. UV–vis measurements were performed to confirm Ag NP formation (Hitachi UV–vis spectrophotometer). The particle size of the synthesized nanoparticles was observed with a TEM instrument (FEI Tecnai G2) operated at an accelerating voltage of 200 kV. The nanofibers as such were deposited on non-carbon-coated copper TEM grids over the aluminum foil in the electrospinning chamber. A small amount of nanofibers was collected on the copper grid during the electrospinning process and then observed under the TEM microscope. The instrument was equipped with an energy-dispersive spectrum (EDS) to confirm the presence of Ag metal in the nanofibers.

Fourier Transform Infrared (FTIR) Spectroscopic Analysis. FTIR analysis was performed for the polymer alone, the Ag NP containing polymeric solution along with the polymer blend solution, and after the addition of PCL, the Ag NP containing polymer solution. The FTIR spectra were obtained by a Thermo-Nicolet spectrometer with KBr pellets in the range 4000–400 cm^{-1}.

X-ray Diffraction (XRD) Analysis. XRD analysis was carried out to study the nanoparticle distribution and crystallinity of the nanoparticle incorporated into the nanofibers. XRD patterns for the nanoparticle-loaded and bare polymer fibers were obtained by a Bruker AXS D8 Advance powder X-ray diffractometer (Cu Kα radiation, $\lambda = 1.5406$ Å) in the range of 10–90° at a scan speed of 0.05°/min.

Field Emission Scanning Electron Microscopy (FESEM) Analysis. The surface morphology of the nanofibers in the electrospun mats were checked with an FESEM instrument (FEI Quanta 200 F, Netherland) operated with an accelerating voltage of 5 kV and a working distance of 20 mm. A small piece of the nanofiber mat was fixed on conductive carbon tape and mounted on the support and then sputtered with an approximately 6-nm layer of gold (Au) for 60 s with a sputter-coating unit (Bal-Tech SC005, Switzerland). The diameter distributions

of the nanofibers in the mats were determined with an Image J tool with sample sizes of at least 50 fibers per scanning electron microscopy (SEM) micrograph. Statistical analysis was performed with Origin Pro 8 software.

Thermogravimetric Analysis (TGA). The as-synthesized nanofibers bulk compositional analysis was carried out by TGA. The nanofibers' susceptibility to higher temperatures, and the effect of the Ag NP incorporation on the stability of the nanofibers was interpreted from thermograms obtained by TGA. About 10 mg of polymeric nanofiber mats were heated from 32 to 600°C at a constant rate of 10°C/min in an EXSTAR TG/DTA 6300. A constant nitrogen atmosphere was maintained throughout TGA of all of the samples. The weight loss of various phases in the thermogram was correlated with the degradation of specific components of the Ag NP loaded nanofibers. The samples were analyzed in perforated and covered aluminum pans under nitrogen-purging conditions.

Suitability of the Scaffold

Atomic Force Microscopy (AFM) Analyses. The surface roughness was determined through the use of AFM. The roughness parameter of a given surface is defined as the centerline average or the distance between the highest and the lowest point of the surface irregularities. Very few nanofibers were deposited on the cover glass, and the dried samples were analyzed by AFM (NTEGRA PNL) in semicontact mode. The images were further processed with NOVA software.

Contact Angle Measurements. Static contact angles of water on the alone PEO–PCL nanofiber and composite nanofiber surfaces were measured with the sessile drop method with a Drop Shape Analysis System-DSA30 (Krüss, Hamburg, Germany). The *contact angle* is defined as the angle at which the liquid interface meets the solid surface of the composite disc at four points on each sample, and the mean of the points was reported as the contact angle of each sample. A volume of 30 μL of ultrapure water was dropped onto the dry nanofibers at 37°C, and the contact angle was calculated after 60 s of incubation time to prevent discrepancy in the contact angle values due to location and time. Bare PEO polymeric nanofibers, PEO–PCL blended nanofibers, and various concentrations of Ag (0.5, 1, 2, and 3 wt %) were studied to better explore the effect of PCL and to understand the effect of the nanoparticles on the fiber wettability.

Silver-Ion Release Study. Silver-ion release behavior from the Ag NP loaded composite nanofiber mats was determined with atomic absorption spectroscopy in the graphite furnace mode (Avanta M, GBC). A small piece of electrospun nanofiber mat (ca. 50 mg) was placed in a 15-mL vial, and 10 mL of phosphate-buffered saline (PBS; pH 7.4) was added to the vial as the release medium. The vial was shaken around 100 rpm and incubated at 37°C. Then, 2 mL of medium was taken at specific time point and replaced by fresh medium to maintain a constant volume.

Antibacterial Application

Antibacterial Assay with the Disc Diffusion Method. The antibacterial activity of the electrospun nanocomposite fibrous mats was evaluated by the disc diffusion method. GFP expressing ampicillin-resistant *E. coli* was used to confirm the antibacterial activity of the nanofibers. The zone of inhibition was analyzed by a qualitative disc diffusion method with 10^7 colony-forming units (cfu) of GFP *E. coli,* which was cultured on LB agar plates. The nanofiber composite membrane discs for study were formed by the deposition of the fibers on a 12-mm glass cover slip. Alone PEO–PCL nanofibers were used as the control, and the Ag NP containing nanofiber composite membranes (1–3 wt %) were used as the test samples. The samples were kept in a Petri plate cultured with GFP *E. coli.* The culture plates were incubated for 12 h at 37°C in the incubator. The zone of inhibition of the microbial colony was observed after the incubation period.

Colony-Counting Method. Various weight amounts (in milligrams) of 2 wt % composite nanofibers were added to different 2-mL LB tubes with 1.5×10^7 cfu of GFP *E. coli.* The mixtures were incubated at 37°C in a shaking incubator for 12 h. A volume of 100 μL of bacterial culture was seeded onto LB agar with a surface-spreading plate technique. The plates were incubated at 37°C for 12 h. All of the experiments were repeated three times, and the results are presented as mean values.

Fluorescence Spectroscopic Analysis. The concentration-dependent antibacterial activity of the composite nanofiber membranes against GFP *E. coli* was investigated by the measurement of the fluorescence of GFP *E. coli* with a Hitachi F-4600 fluorescence spectrophotometer (excitation = 410 nm).

Fluorescence Microscopic Analysis. For fluorescence microscopic analysis, 5 μL of the composite nanofiber-treated and untreated GFP *E. coli* bacterial samples were placed over microscope slides to form a thin smear and were then viewed after air-drying with a Nikon Eclipse LV100 microscope attached to a B-2A filter at an excitation wavelength of 445–495 nm.

FESEM Analysis. To study the fine topological changes on the bacterial membrane due to the bactericidal activity of the alone PEO–PCL nanofibers and composite nanofiber membranes, discs were investigated by the inoculation of 10^7 cfu/mL GFP *E. coli* on fibers for 12 h under shaking conditions at 37°C. After overnight incubation, the nanofibers were taken out and washed with PBS several times to remove any excess bacteria. The remaining cells adhered to nanofibers were fixed by the addition of the proper amount of PBS containing 3% glutaraldehyde. Then samples were washed again with ethanol and finally air-dried at 37°C.

Statistical Analysis. The data were expressed as the mean plus or minus the standard deviation of one or more individual experiments wherever applicable. The analysis of data was performed with the Student's *t* test with GraphPad Prism 6.0, and the statistically significant values were indicated as follows: $^{*}p < 0.05$, $^{**}p < 0.005$, and $^{***}p < 0.001$.

RESULTS AND DISCUSSION

Microscopic and Spectroscopic Analysis of Ag NPs Synthesized in a Polymeric Solution

Generally, the synthesis of Ag NPs (Ag^0) from $AgNO_3$ (Ag^+) requires reducing agents, such as sodium borohydrate and

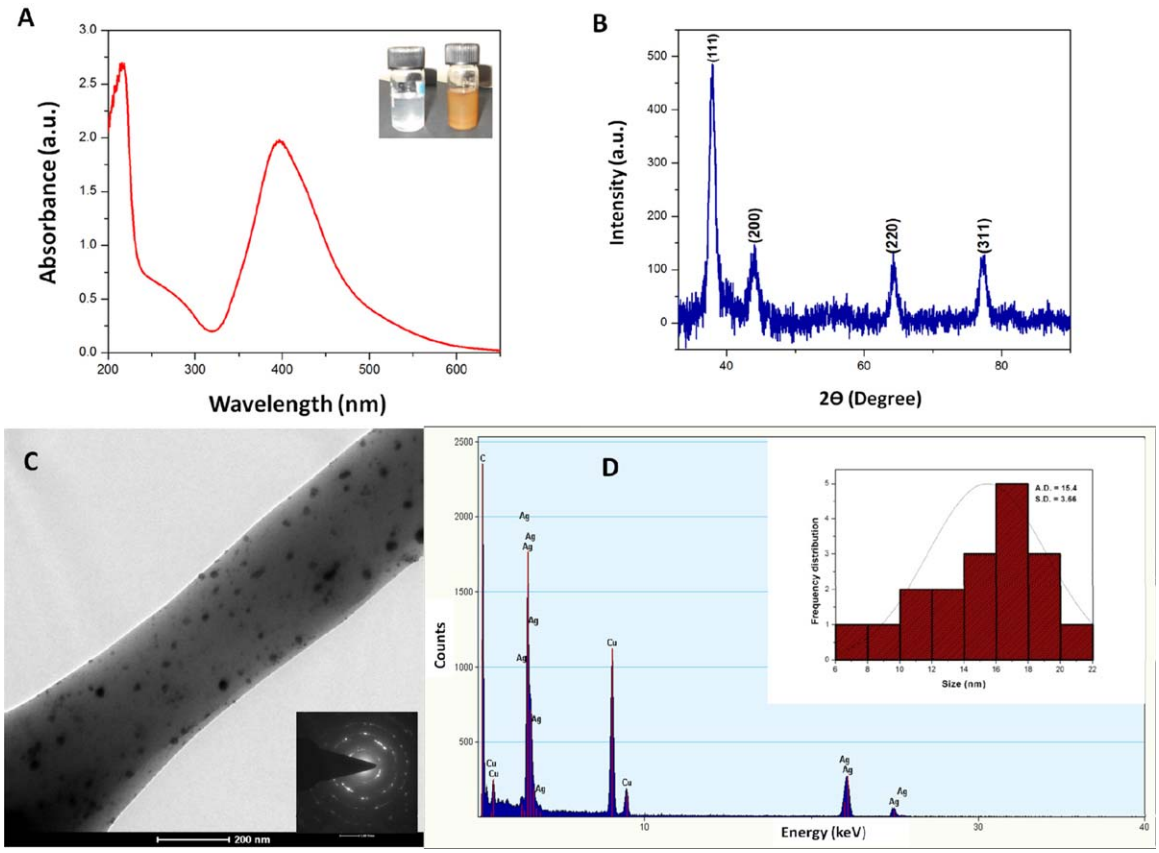

Figure 1. (A) UV–vis spectrum of the as-synthesized Ag NPs in PEO solutions. The inset shows the PEO solution before and after the synthesis of the Ag NPs. (B) Typical XRD pattern of the as-synthesized Ag NPs in a PEO solution. (C) TEM images of the Ag NP loaded composite nanofiber. The inset shows the corresponding selected area electron diffraction (SAED) pattern. (D) Energy dispersive X-ray analysis (EDAX) spectrum and elemental composition of the nanofiber obtained with TEM. The inset shows the histogram for the size distribution of the nanoparticles. [Color figure can be viewed in the online issue, which is available at wileyonlinelibrary.com.]

vitamin C, and a stabilizing agent, such as a polymer, citrate, or protein; this prevents the aggregation of particles. Here, we explored a method where the polymer solution itself acted as stabilizing and reducing agents, and this was in agreement with a previous report.[1] The same polymer solution was further taken for the electrospinning process. It was reported in the recent past that high-molecular-weight PEO polymer reduces Ag^+ ions to Ag NPs under certain experimental conditions.[19] It was also reported that DMF reduces Ag^+ salt to Ag NPs.[20] Thus, by combining these two approaches, we explored a simple method for the synthesis of Ag NPs without the use of any further addition of reducing and stabilizing agents, which could be toxic to cells. The Ag NPs were well incorporated and dispersed in biodegradable and biocompatible polymeric nanofibers. The optical properties of the Ag NPs in the polymer were analyzed by absorption spectroscopy. The plasmon absorption peak around 390–400 nm was characteristic of nanosize Ag NPs; this was adequate for confirming the formation of the particles [Figure 1(A)]. The UV–vis spectrum displayed the characteristic peak of Ag NPs. This result was consistent with the TEM image. The average particle size obtained from TEM was 15 ± 2 nm [Figure 1(C)]. Further, the presence of elemental silver was confirmed by TEM energy dispersive X-ray analysis (EDAX) analysis [Figure 1(D)]. All of the previous characterization methods confirmed the successful synthesis of crystalline and well-dispersed stable Ag NPs.

XRD Elemental Analysis

The structural properties and crystalline behavior of the Ag NPs in the polymeric blended composite nanofibers were explored by the powder XRD. The resulting diffraction patterns were analyzed by PaNalytical X'Pert High Score Plus software. The characteristic peaks of elemental Ag were shown at $2\theta = 38.1$, 44.0, 64.23, and 77.1° represented Ag (111), Ag (200), Ag (220), and Ag (311), respectively [Figure 1(B)], and these four facial diffraction peaks were in agreement with JCPDS 040783. The XRD patterns confirmed that the polymeric blend was semicrystalline in nature and also confirmed the presence of Ag as Ag NPs in the composite nanofibers, where the crystal structure of Ag was a surface cubic crystal structure.

Electrospinning of the Composite Nanofiber Solutions

Fabrication of PEO and PCL nanofibers has been reported by many researchers because they have several advantages. PEO nanofibers have been studied for wound-dressing applications along with some other polymers and drug molecules.[21–23] PCL has been used in drug-delivery systems[24–26] and has been widely used in polymeric blends because it provides mechanical

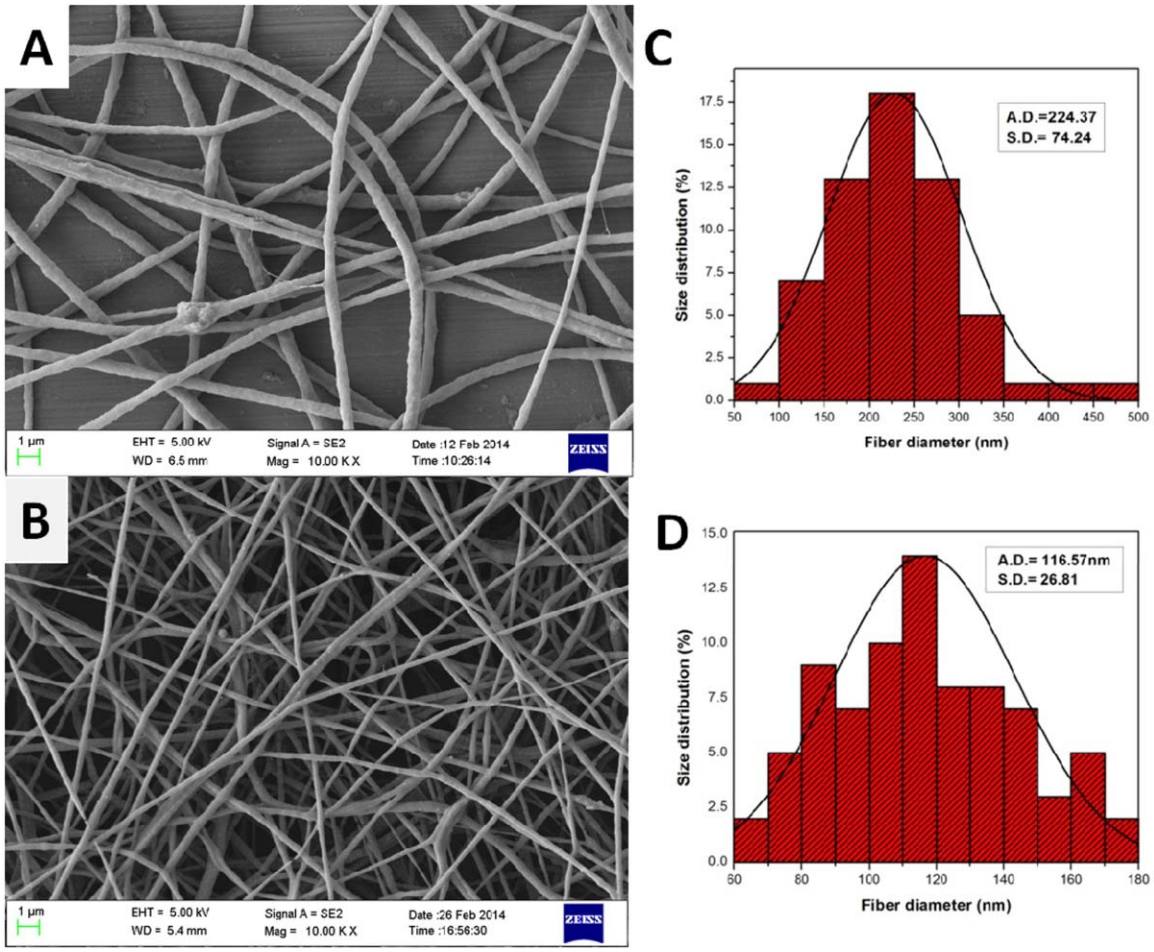

Figure 2. FESEM observations of the (A) PEO–PCL blended nanofiber alone and (B) Ag NP loaded composite nanofibers. Histograms of the (C) PEO–PCL blended nanofiber alone and (D) Ag NP loaded composite nanofibers showing the nanofiber distribution (S.D. = standard deviation; A.D. = average diameter). [Color figure can be viewed in the online issue, which is available at wileyonlinelibrary.com.]

strength. PEO–PCL incorporated curcumin block copolymeric nanofibers were synthesized recently.[27] Other water-soluble polymers used for the fabrication of nanofibers with Ag NPs require crosslinking agents such as glutaraldehyde vapor, which can be toxic for cells. In contrast, the nanofibers fabricated with PEO–PCL blended nanofibers do not require any crosslinking agent as the combination of hydrophilic and hydrophobic polymeric mixture makes the composites significantly hydrophobic and thus stable. Fiber formation was optimized by the variation of the flow rate, voltage, and tip-to-collector distance along with solution parameters, such as viscosity and concentration. For the proper synthesis of the composite nanofibers, the order of dissolution was also important, as $AgNO_3$ is soluble in DMF but not in DCM, and DCM/DMF is miscible among them. Beaded fibers were formed at very low concentrations of polymeric solution (1 wt % PEO). Thus, the optimum concentration (3–4 wt % PEO and 1–2 wt % PCL) was used for fiber formation. At slightly higher concentrations (5 wt % of PEO and 4 wt % of PCL), the solution became so viscous that it could not be injected. The selected concentration was further taken for the formation of Ag NP containing PEO–PCL blended nanofibers with a need for the optimization of voltage as Ag is a metal and is conducting in nature. Thus, there was a need for the optimization of Ag NP concentration, voltage, and tip-to-collector distance for beadless fiber formation. Three concentrations of Ag NPs, 1, 2, and 3 wt %, were used for fiber formation. Compared to bare fibers, the composite nanofibers showed smaller fiber diameters. The reason could have been the presence of charge-conducting metal in the composite nanofibers. The alone PEO–PCL nanofibers were obtained at an average diameter in the range 150–300 nm [Figure 2(A,C)], whereas all of the other composite fibers showed fiber diameters of 70–150 nm [Figure 2(B,D)].

Microscopic and Spectroscopic Observations of the Nanofibers

SEM and TEM images of the Ag NP embedded polymeric nanofibers [Figures 1(C) and 3(B)] were taken, and Image J software was used to measure the size of the nanofibers. The polymer nanofibers were 150–300 nm in diameter, whereas the nanofibers with Ag NPs were about 70–150 nm in diameter, as observed in the SEM image. The Ag NP containing nanofibers had a rough surface morphology along with porosity when compared to the control nanofibers; this indicated that Ag NPs

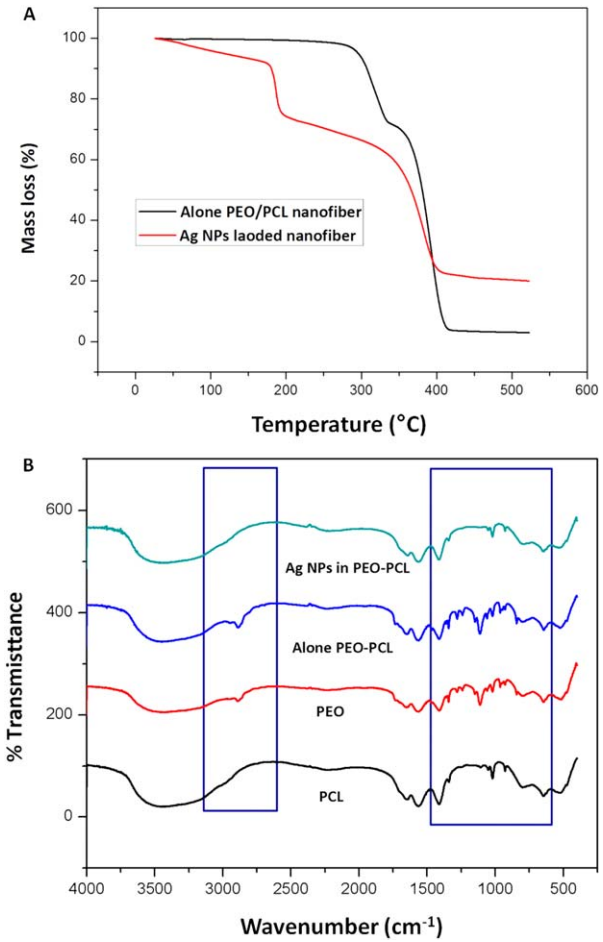

Figure 3. (A) TGA of nanofibers (B) FTIR spectrogram of Ag NPs synthesized in a polymer solution. [Color figure can be viewed in the online issue, which is available at wileyonlinelibrary.com.]

were not only incorporated into but were also present on the surface of the nanofibers. The TEM image clearly showed the formation of stable, spherical, and dispersed nanoparticles in the polymeric matrices, and the size of the particles varied from 15–20 nm; this corroborated with the UV–vis spectrum [Figure 1(A)].

FTIR Spectroscopic Measurement

The characteristic FTIR spectrum of the Ag NPs synthesized in PEO solution and the effect of further addition of PCL solution were observed [Figure 3(B)]. We interpreted that the probable reason for the formation of Ag NPs in solution could have been a partial reduction of Ag^+ ions by the presence of the aldehyde group (—CHO) in PEO and DMF molecules present in solution. The interaction of electropositive Ag^+ ions with the electron-rich oxygen atom of hydroxyl (—OH) and —CHO group resulted in electrostatic (i.e., ion–dipole) interactions. Further, the stabilization of nanoparticles was indicated by the presence of high-molecular-weight PEO molecules. The formation of Ag NPs was observed by changes in the color of the solution from white to yellow because of the surface plasmon resonance phenomena; this could have been the result of previous interactions in the solution.

The IR spectral analysis of the 4 wt % pure PEO polymer solution, 1 wt % PCL, PEO–PCL blend solution containing Ag NPs, and PEO solution containing Ag NPs was done. We observed that all of the major peaks were present for the PEO and PCL solutions; for example, C—H stretching mode was observed at 2876 cm^{-1}, CH_2 scissoring mode was observed at 1466 cm^{-1}, CH_2 wagging mode was observed at 1360 and 1341 cm^{-1}, CH_2 twisting mode was observed at 1279 cm^{-1}, C—O—C stretching was observed at 1104, CH_2 rocking and C—O—C vibration mode were observed at 960 cm^{-1}, CH_2 rocking was observed at 841 cm^{-1}, and C—O—C bending was observed at 528 cm^{-1}. However, the semicrystalline phase of PEO was confirmed by the presence of a triplet peak of C—O—C stretching vibrations at 1145, 1095, and 1059 cm^{-1}, with the maximum intensity at 1095 cm^{-1}[128] disappearing along with the peak at 2876 cm^{-1} in solution after the formation of Ag NPs. The complexation of silver salt with PEO was confirmed by the appearance of the peak at 636 cm^{-1}.[29]

Thermal Properties of the Nanofiber Membranes

TGA of the alone PEO–PCL nanofibers and composite nanofiber (2%) nanofibrous sheets was done at a heating rate of 10°C/min and at temperatures up to 400°C [Figure 3(A)]. The results show that there was no weight loss up to 160°C. The weight loss mainly occurred in the temperature range from 160 to 360°C with a negligible change at temperatures higher than 360°C. This weight loss indicated thermal decomposition or evaporation in the material. As shown in the figure, it was clear that the specimen's weight loss occurred mainly because of the combustion of the organic PEO–PCL matrix. The TGA results shown in Figure 3(A) also indicate that the degradation temperature of the composite nanofiber decreased and the weight loss increased in the presence of Ag NPs. This means that the thermal stability of the nanofibrous sheets was decreased because of the presence of Ag NPs in the nanofibers.[30] The probable explanation for this was attributed to the high thermal conductivity of Ag NPs compared to the polymeric nanofibers.[30]

Suitability of the Scaffold

Roughness Analysis. The different surface roughness is a requisite for the adherence and growth of different cell lines. For instance, a study by Xu *et al.*[31] proved that vascular endothelial cell function was enhanced on a smooth solvent cast surface rather than on the rough electrospun surface of poly(L-lactic acid). Thus, it is one of the important parameters in biomaterials that affects the cell behavior; thus, the surface roughness should be considered in the design of the scaffold for biomedical applications.[31] AFM was used to determine the surface roughness of the nanofibers, and we observed that the surface roughness of the composite nanofibers was greater than that of the alone PEO–PCL nanofibers [Figure 4(A,B)]. The probable reason for the previous observation was the presence of Ag NPs on the surface of the nanofibers. This study was in agreement with the FESEM analysis.

Hydrophilicity and Wettability Analysis. It is desirable to check the wettability of biomaterials when one intends to produce materials for biomedical applications, such as scaffolds for cellular proliferation, wound healing, or skin tissue

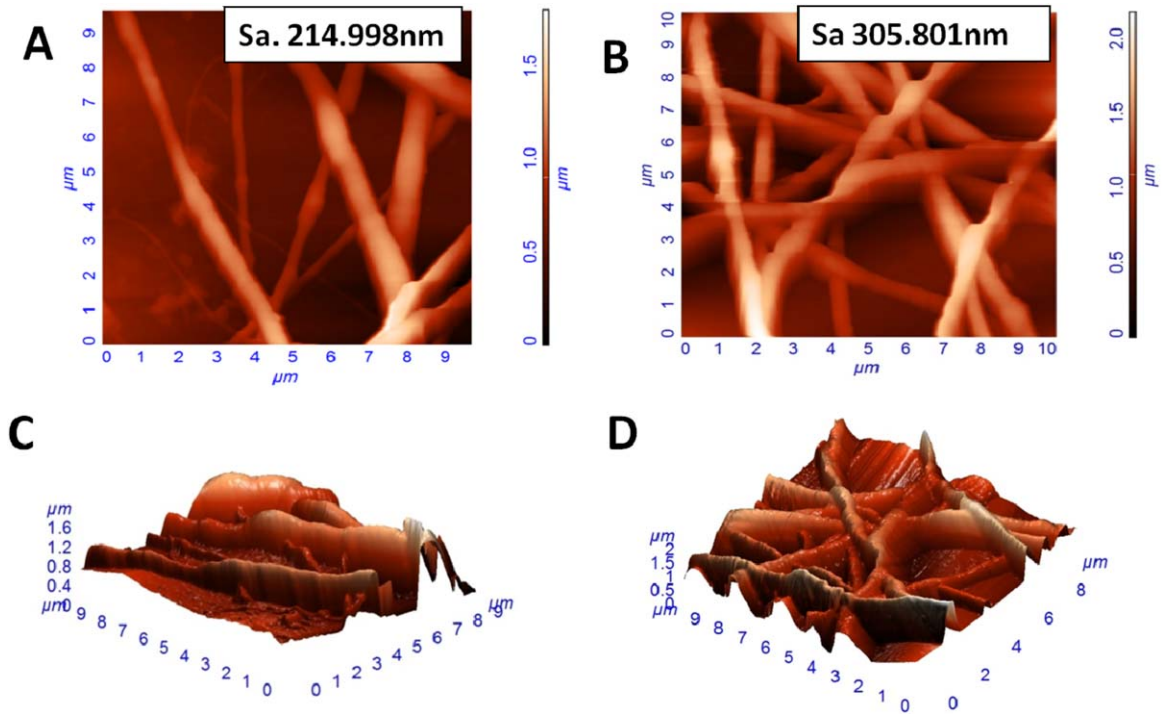

Figure 4. Roughness analysis of the (A) PEO–PCL blended nanofiber alone and (B) composite nanofiber. (C,D) Corresponding three-dimensional structures by AFM (Sa = surface roughness). [Color figure can be viewed in the online issue, which is available at wileyonlinelibrary.com.]

engineering,[32] as they will come into contact with blood, water, and other body fluids during their use. Water contact angle measurement is an accepted way to investigate the membrane surface hydrophilicity. It provides a clear idea about the nature of the scaffold surface, whether it is hydrophilic or hydrophobic.[32] One can do this by checking the contact angle between a liquid and the surface of the electrospun matrix. In our study, because of the inherent hydrophilic nature of the base polymer PEO used for Ag NP synthesis, there was a need to blend it with a hydrophobic polymer, such as PCL, as the wettability of the electrospun hydrophilic scaffolds could be tailored through the introduction of hydrophobic polymers. As PCL is well known for its hydrophobicity, 1 wt % PCL was added to the blend. Through the addition of PCL, there was a significant increase in the hydrophobicity of the fibers, as shown in Figure 5(B), compared to PEO alone [Figure 5(A)]. It was reported in the literature that the wound-healing performance is mainly influenced by the air permeability, porosity, and wettability of

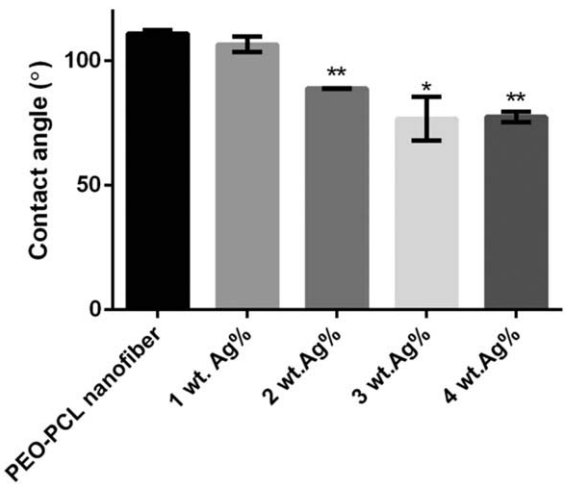

Figure 5. Contact angle (wettability) measurements for the PEO–PCL nanofiber alone and the composite PEO–PCL nanofibers with 1, 2, 3, or 4 wt % Ag. $^{*}p < 0.05$, $^{**}p < 0.005$, and $^{***}p < 0.001$.

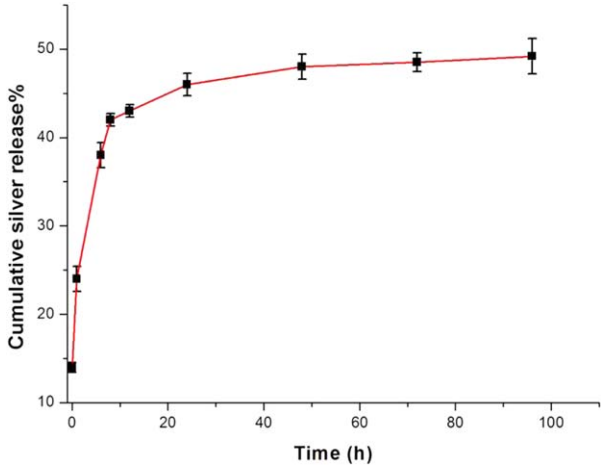

Figure 6. *In vitro* silver-ion release study of the Ag NP incorporated composite nanofibers at a physiological pH of 7.4 in a PBS buffer solution for 96 h. [Color figure can be viewed in the online issue, which is available at wileyonlinelibrary.com.]

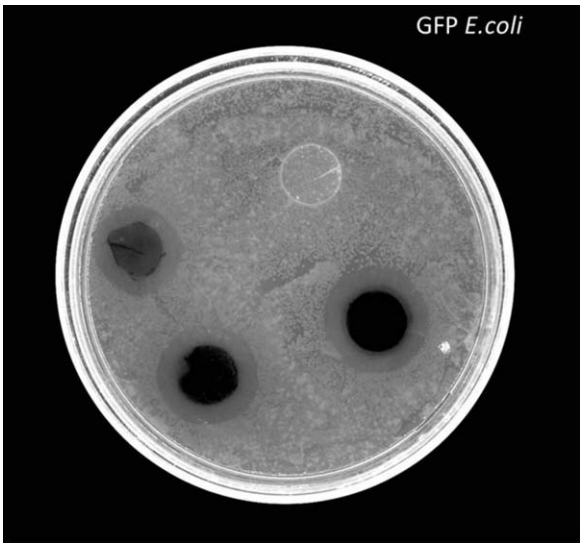

Figure 7. Antibacterial disc diffusion assay showing a zone of inhibition against Gram-negative recombinant GFP *E. coli* for 1, 2, and 3 wt % Ag composite nanofibers.

the surface of the nanofiber membranes. A nanofiber membrane with good hydrophilicity and high porosity facilitates wound healing considerably, especially in the early healing stage.[33] In this study, the initial contact angle was adopted to confirm the hydrophilicity modification of membrane surface with PCL and Ag NPs. Interestingly, the contact angle values of all of the composite nanofibers shown in Figure 5(C,D) were dramatically lower than those of the original membrane, which lacked silver [Figure 5(B)]; this indicated that Ag NPs were capable of significantly enhancing the surface hydrophilicity of the membrane. There was no significant decrease in the contact angle [shown in Figure 5(E,F)]; this was probably due to high chances of aggregation of Ag NPs on the membrane surface at a relatively high concentration of $AgNO_3$.;[34] The probable explanation for the improvement of the membrane hydrophilicity is as follows. Ag NPs released Ag^+ ions in the aqueous phase by oxidation; these could simultaneously be adsorbed onto the Ag NP surface in the formation of hydrated Ag^+ ions;[35] this could have possibly been the source of the Ag NP hydrophilicity. This was also supported by a recent study done by Li *et al.*[35]

Silver-Ion Release

The sustainability of Ag NPs in the PEO–PCL nanofibers was investigated by *in vitro* drug-release profiles under physiological conditions at different time points. The release rate of the encapsulated Ag NPs showed an initial burst release for the period of 24 h; this was followed by a continuous slow and sustained release (Figure 6). During the period of 96 h of incubation, around half (51%) of the encapsulated Ag NPs were released from the nanofibers. The initial burst release of Ag NPs was possibly due to the diffusion of Ag NPs that were adsorbed at the surface of the polymeric nanofibers. However, the sustained release of Ag NPs in subsequent stages may have been due to the diffusion of encapsulated Ag NPs from the core region of the polymeric nanofibers or may have been based on the degradation of PEO from the polymeric matrix. The results obtained were in agreement with Wu *et al.*[36] and indicated that these nanofibers could be potentially useful for the sustained delivery of Ag NPs for long-term wound-dressing applications.

Estimation of the Antibacterial Efficacy

The agar disc diffusion method (Kirby–Bauer) is a relatively facile and quick semiquantitative approach for determining the antibacterial activity of diffusible antimicrobial agents from various drug-delivery systems. The disc diffusion tests showed an exclusion area around the composite nanofiber discs, whereas

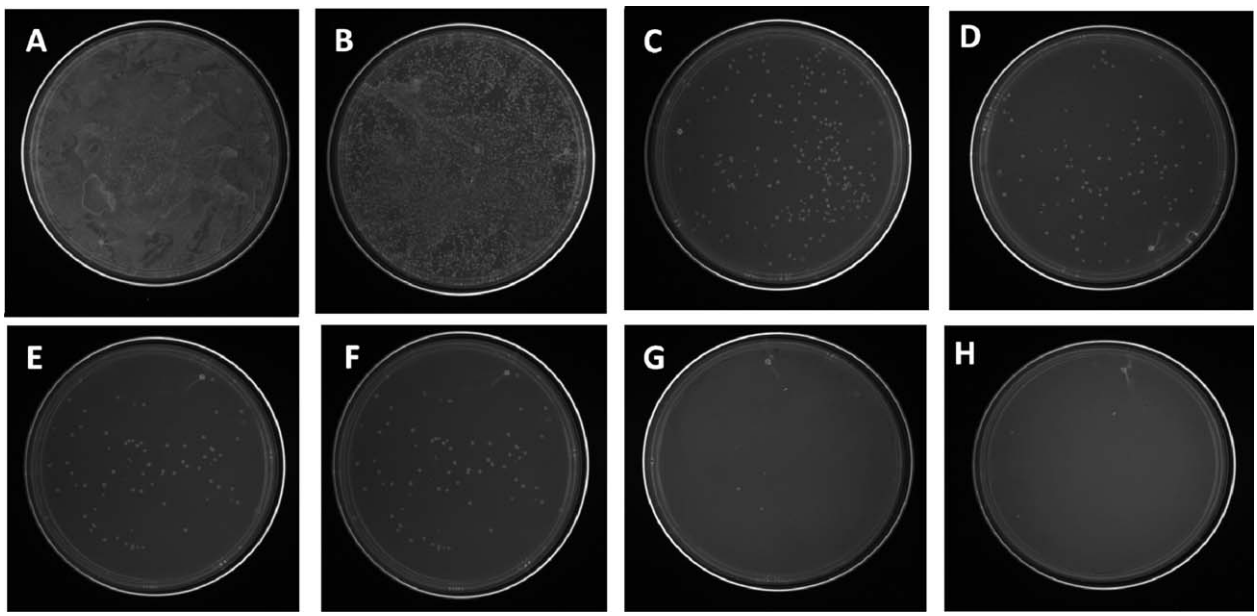

Figure 8. Effects of different concentrations of nanofibers on the viability of antibiotic-resistant GFP *E. coli*: (A) PEO–PCL nanofiber$_{\text{-treated}}$ cells alone and (B–H) composite nanofiber-treated cells of various weights (0, 1, 2, 4, 6, 7, 8, and 10 mg).

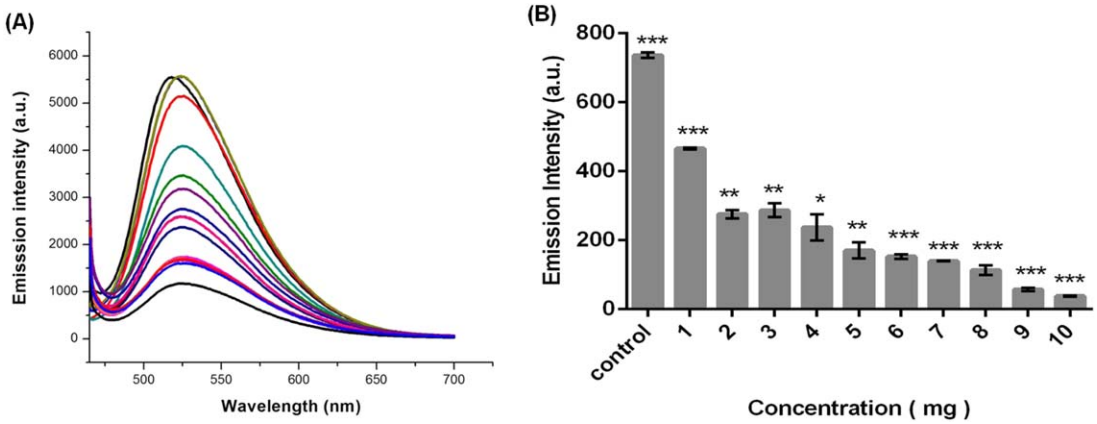

Figure 9. (A) Fluorescence spectra (excitation wavelength = 410 nm) depicting GFP *E. coli* treated with different concentrations of nanofibers. (B) Histogram presenting the value of the fluorescence intensity at 525 nm specific for the GFP protein. $^{*}p < 0.05$, $^{**}p < 0.005$, and $^{***}p < 0.001$. [Color figure can be viewed in the online issue, which is available at wileyonlinelibrary.com.]

the alone PEO–PCL nanofibers were kept as the control. Composite nanofibers were used for the antibacterial assessment of various concentrations (1, 2, and 3 wt %) of Ag NPs in the fibers. A zone of inhibition appeared immediately after 4 h; this clearly showed a strong antibacterial effect of the membrane discs, and the maximum activity of the membranes until 12 h of incubation was assessed (Figure 7). The result shows that the Ag NP containing composite membranes exhibited significant toxicity against the antibiotic-resistant GFP *E. coli* bacteria.

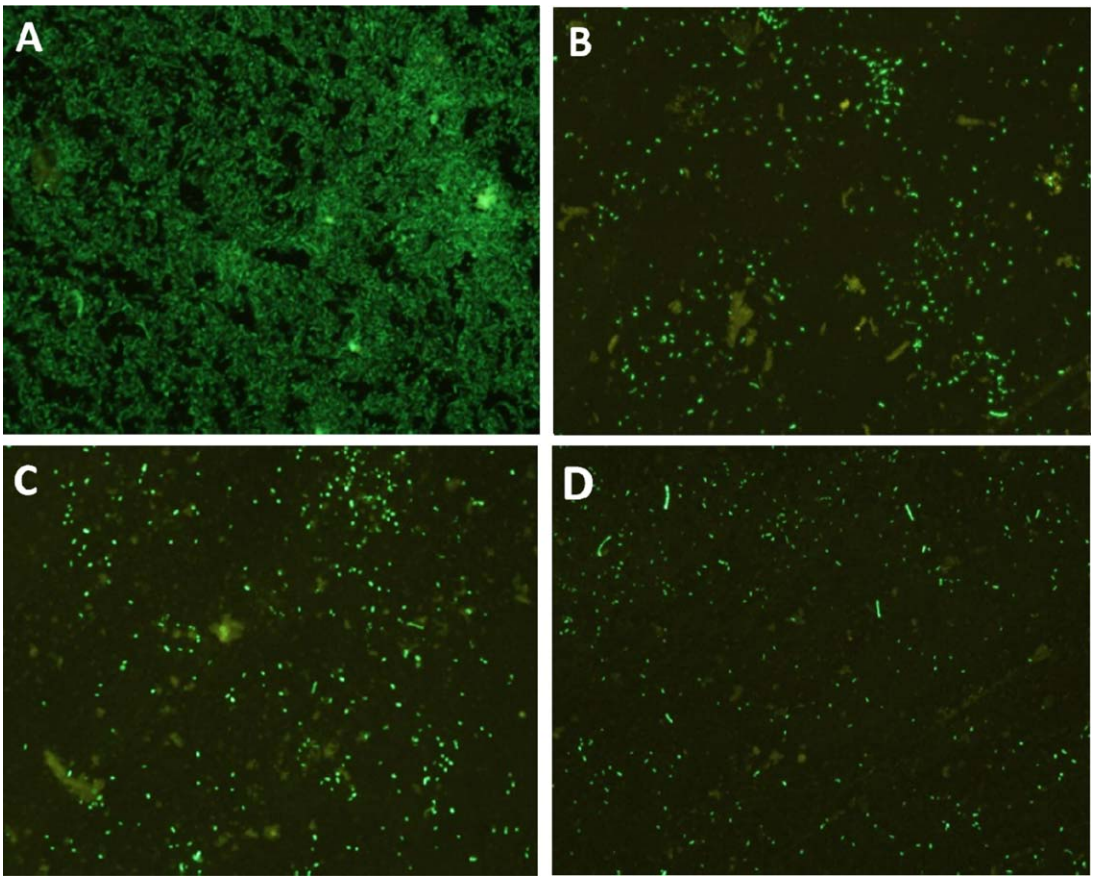

Figure 10. Fluorescence micrographic images of GFP *E. coli* treated with different concentrations of nanofibers: (A) PEO–PCL nanofiber alone and (B–D) composite nanofibers with various concentrations (1, 5, 7, and 10 mg). All images were taken at a magnification of 20×. [Color figure can be viewed in the online issue, which is available at wileyonlinelibrary.com.]

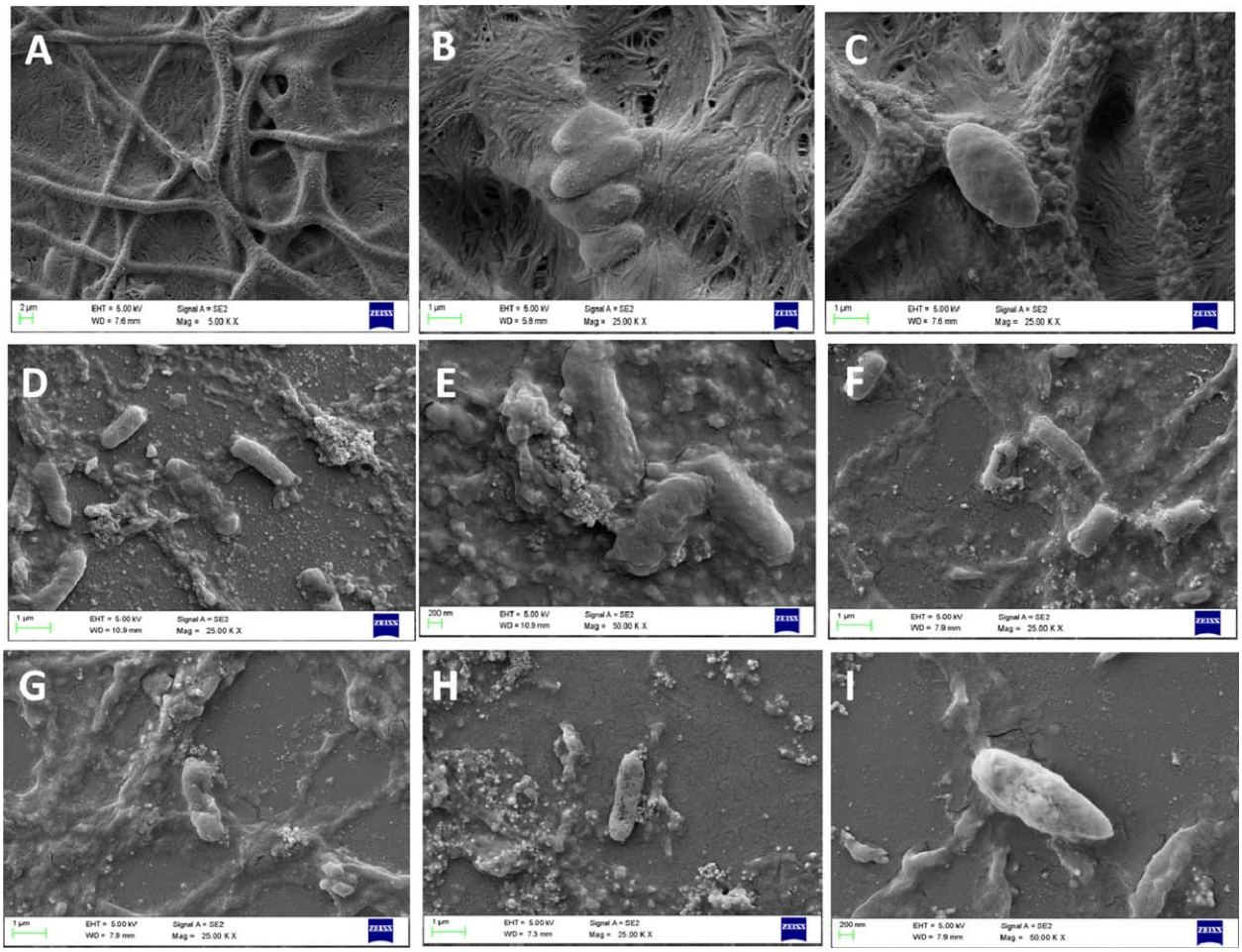

Figure 11. FESEM micrographs of GFP *E. coli* seeded over the (A–C) PEO–PCL nanofiber alone and (D–I) composite nanofiber. [Color figure can be viewed in the online issue, which is available at wileyonlinelibrary.com.]

Evaluation of the Antibacterial Effect by the cfu Method

It is one of the reliable methods for assessing the antibacterial potential of an antibacterial agent. In this study, distinguishable colonies (even with <1 mg composite nanofiber treatment) were observed on the plates; they could be counted manually when compared to the lawn of colonies on the control plate. This clearly showed significant growth inhibition of the bacteria by the nanofibers. We found that when we increased the weight of the composite nanofibers, a significant amount of bacterial cells decreased, and when compared to the control plate, the colonies were almost negligible around a weight of 10 mg of the composite nanofibers (Figure 8).

Fluorescence Spectroscopic and Microscopic Analysis

The expression of GFP protein in *E. coli* cells facilitates rapid monitoring of the antibacterial phenomena of composite nanofibers by spectroscopic and microscopic techniques. The fluorescence spectral studies revealed a continual decrease in the fluorescence of GFP *E. coli* with increasing concentration of the composite nanofiber [Figure 9(A,B)]. A strong green emission band at 510 nm was observed in the untreated bacteria; this is a characteristic feature of live GFP *E. coli*. No fluorescence was observed in GFP *E. coli* treated with 10 or 12 mg of composite nanofibers; this suggested complete eradication of bacteria at these concentrations. Fluorescence microscopic images (20× magnification) of GFP *E. coli* treated with different concentrations (1, 5, 7, and 10 mg) of composite nanofibers are depicted in Figure 10(A–D). A significant decrease in the GFP *E. coli* bacterial count was visualized with increasing weight (in milligrams) of composite nanofibers. When the weight amount of composite nanofibers was increased from 1 to 10 mg, a steady decrease in the size and population of bacteria was observed as compared to the alone PEO–PCL nanofiber-treated bacteria, as shown in Figure 10. The obtained fluorescence microscopic images correlated well with the fluorescence spectroscopic measurements; this suggested strong antibacterial effects of the as-synthesized composite nanofibers against GFP expressing antibiotic-resistant *E. coli*.

Morphological Observation of the Treated Bacterial Cells by FESEM

FESEM analysis of the nanofibers (alone PEO–PCL and Ag NP incorporated composite nanofiber) seeded with bacterial

cells clearly showed the deformation of the bacterial cell morphology and the complete degradation of the GFP *E. coli* bacterial cell wall by the penetration of Ag NPs into the bacterial cells after treatment with composite nanofiber membranes for period of 12 h. The probable reason for the binding of nanoparticles to the bacterial proteins the generation of ROS, which ultimately led to cell death, as reported in many articles,[17] whereas the morphology of bacterial cells remained intact after treatment with the alone PEO–PCL nanofibers, which lacked nanoparticles (Figure 11), after 12 h of incubation.

CONCLUSIONS

Successful fabrication of the PEO–PCL nanofiber mats was done by the blending electrospinning technique. Ag NPs with an average size of 15–20 nm were synthesized and characterized well by various techniques. The composite nanofibrous membranes with 1, 2, 3, and 4 wt % were prepared, and we found that the fiber diameter decreased slightly from 224 to 116 nm because of the addition of charged particles. Thermal studies showed that Ag NP incorporation altered the thermal stability of the alone PEO–PCL loaded nanofibers to a higher extent because of the formation of the composite nanofibers; this was further supported by literature. The suitability of the scaffold is an important parameter in the consideration of biomedical usage. Thus, surface roughness and wettability analyses were performed, and the results were in good agreement with the previously reported data for ideal wound-dressing scaffolds. Antibacterial studies demonstrated the concentration-dependent inhibition of bacterial growth. Various other antibacterial assays, such as quantitative assays, were performed and confirmed the bactericidal activity of the scaffold. Morphological examination clearly showed bacterial death after treatment with the Ag NP incorporated nanofibers. Hence, a judicial choice of the concentration of Ag NPs needs to be identified for *in vivo* applications to ensure less toxicity and maximum antibacterial activity.

ACKNOWLEDGMENTS

The authors sincerely thank the Science and Engineering Research Board (contract grant number SR/FT/LS-57/2012) and the Department of Biotechnology (contract grant number BT/PR6804/GBD/27/486/2012) of the Government of India for the financial support. Five of the authors (P.D., B.B., A.S., I.M., and S.U.K.) are thankful to the Ministry of Human Resource Development of the Government of India for a fellowship. The Department of Chemistry and the Institute Instrumentation Centre of the Indian Institute of Technology Roorkee are sincerely acknowledged for providing various analytical facilities.

REFERENCES

1. Shalumon, K. T.; Anulekha, K. H.; Nair, S. V.; Chennazhi, K. P.; Jayakumar, R. *Int. J. Biol. Macromol.* **2011**, *49*, 247.
2. Murugan, R.; Ramakrishna, S. *Tissue Eng.* **2006**, *12*, 435.
3. Abrigo, M.; McArthur, S. L.; Kingshott, P. *Macromol. Biosci.* **2014**, *14*, 772.
4. Gogoi, S. K.; Gopinath, P.; Paul, A.; Ramesh, A.; Ghosh, S. S.; Chattopadhyay, A. *Langmuir* **2006**, *22*, 9322.
5. Sahni, G.; Gopinath, P.; Jeevanandam, P. *Colloids Surf. B* **2013**, *103*, 441.
6. Chen, J.-P.; Chiang, Y. *J. Nanosci. Nanotechnol.* **2010**, *10*, 7560.
7. Hong, K. H.; Park, J. L.; Sul, I. H.; Youk, J. H.; Kang, T. J. *J. Polym. Sci. Part B: Polym. Phys.* **2006**, *44*, 2468.
8. Rujitanaroj, P.-O.; Pimpha, N.; Supaphol, P. *J. Appl. Polym. Sci.* **2010**, *116*, 1967.
9. Xu, X.; Zhou, M. *Fibers Polym.* **2008**, *9*, 685.
10. Li, C.; Fu, R.; Yu, C.; Li, Z.; Guan, H.; Hu, D.; Zhao, D.; Lu, L. *Int. J. Nanomed.* **2013**, *8*, 4131.
11. Fouda, M. M. G.; El-Aassar, M. R.; Salem, S. A.-D. *Carbohydr. Polym.* **2013**, *92*, 1012.
12. Abdelgawad, A. M.; Hudson, S. M.; Rojas, O. *J. Carbohydr. Polym.* **2013**, *100*, 107.
13. Yoshii, F.; Zhanshan, Y.; Isobec, K.; Shinozaki, K.; Makuuchi, K. *Radiat. Phys. Chem.* **1999**, *55*, 133.
14. Merrell, J. G.; McLaughlin, S. W.; Tie, L.; Laurencin, C. T.; Chen, A. F.; Nair, L. S. *Clin. Exp. Pharmacol. Physiol.* **2009**, *36*, 1149.
15. Gliga, AR.; Skoglun, S.; Wallinder, I. O.; Fadeel, B.; Karlsson, BL. *Part. Fibre Toxicol.* **2014**, *11*, 11.
16. Poornima, D.; Ishita, M.; Kumar, US.; Abhay, S.; Bharat, B.; Gopinath, P. *Adv. Colloid Interface Sci.* **2015**. DOI: 10.1016/j.cis.2015.02.007.
17. Matai, I.; Sachdev, A.; Dubey, P.; Kumar, S. U.; Bhushan, B.; Gopinath, P. *Colloids Surf. B* **2014**, *11*, 5359.
18. Pillay, V.; Dott, C.; Choonara, Y. E.; Tyagi, C.; Tomar, L.; Kumar, P.; du Toit, L. C.; Ndesendo, V. M. K. *J. Nanomaterials* **2013**, *2013*, 22.
19. Saquing, J.; Manasco, L.; Khan, S. A.; Carl, D. *Small* **2009**, *5*, 944.
20. Pastoriza-Santos, I.; Liz-Marzán, L. M. *Pure Appl. Chem.* **2000**, *72*, 83.
21. Gatti, J. W.; Smithgall, M. C.; Paranjape, S. M.; Rolfes, R. J.; Paranjape, M. *Biomed. Microdevices* **2013**, *15*, 887.
22. Xie, Z.; Paras, C. B.; Weng, H.; Punnakitikashem, P.; Su, L.-C.; Vu, K.; Tang, L.; Yang, J.; Nguyen, K. T. *Acta Biomater.* **2013**, *9*, 9351.
23. Doğan, G.; Özyıldız, F.; Başal, G.; Uzel., A. *Int. Polym. Process.* **2013**, *28*, 143.
24. Wang, Y.; Wang, B.; Qiao, W.; Yin., T. *J. Pharm. Sci.* **2010**, *99*, 4805.
25. Jia, Y. T.; Liu, Q.; Zhu, X. *Adv. Mater. Res.* **2011**, *9*, 1235.
26. Amn, T.; Barakat, N. A. M.; Hassan, M. S.; Khil, M.-S.; Kim, H. Y. *Colloids Surf. A* **2013**, *431*, 1.
27. Guo, G.; Fu, S. Z.; Zhou, L. X.; Liang, H.; Fan, M.; Luo, F.; Qian, Z. Y.; Wei, Y. Q. *Nanoscale* **2011**, *3*, 3825.
28. Islam, A. K. M. M.; Mukherjee, M. *J. Exp. Nanosci.* **2011**, *6*, 596.
29. Shameli, K.; Ahmad, M. B.; Jazayeri, S. D.; Sedaghat, S.; Shabanzadeh, P.; Jahangirian, H.; Mahdavi, M.; Abdollahi, Y. *Int. J. Mol. Sci.* **2012**, *13*, 6639.

30. Almajhdi, N. F. H.; Abdelrazek, F. K.; Awad, K. H. M.; Mohamed, S. H. S.; Ahmed, T. E.; Fawzi, M. A.; Al-Jassir, F.; Abdo, H. S. *J. Mater. Sci. Mater. Med.* **2014**, *4*, 1045.

31. Xu, C.; Yang, F.; Wang, S.; Ramakrishna, S. *J. Biomed. Mater. Res. A* **2004**, *71*, 154.

32. Ghosal, K.; Thomas, S.; Kalarikkal, N.; Gnanamani, A. *J. Polym. Res.* **2014**, *21*, 410.

33. Liu, J. Y.; Hurt, R. *Environ. Sci. Technol.* **2010**, *44*, 2169.

34. Yuliwati, E.; Ismail, A. F.; Matsuura, T.; Kassim, M. A.; Abdullah, M. S. *Desalination* **2011**, *283*, 214.

35. Li, J.-H.; Shao, X.-S.; Zhou, Q.; Li, M.-Z.; Zhang, Q.-Q. *Appl. Surf. Sci.* **2013**, *265*, 663.

36. Wu, J.; Zheng, Y.; Song, W.; Luan, J.; Wena, X.; Wu, Z.; Chen, X.; Wang, Q.; Guo, S. *Carbohydr. Polym.* **2014**, *102*, 762.